ADHESIVE BONDED COMPOSITE LAMINATE DOUBLE LAP JOINT AND PROGRESSIVE FAILURE ANALYSIS

Jeong Sik Kwon[1], Dong Guk Choi[2], Jung Sun Park[3], and Soo Yong Lee[4]

[1]Department of Aerospace & Mechanical Engineering, Korea Aerospace University, Goyang-si 412-791, Republic of Korea
youngaircraft@gmail.com
[2]Department of Aerospace & Mechanical Engineering, Korea Aerospace University, Goyang-si 412-791, Republic of Korea
codnkk@naver.com
[3]Department of Aerospace & Mechanical Engineering, Korea Aerospace University, Goyang-si 412-791, Republic of Korea
jungsun@kau.ac.kr
[4]Department of Aerospace & Mechanical Engineering, Korea Aerospace University, Goyang-si 412-791, Republic of Korea
leesy@kau.ac.kr

Keywords: ASTM D3528, Progressive Failure Analysis (PFA), Adhesive Properties, Laminate Failure Theory

Abstract

A comprehensive procedure for adhesive bonded composite laminate joint (ASTM D3528 Proc. B) is demonstrated by a failure analysis of test results. Tests were perform on the ASTM D5656 to characterize the adhesive shear properties for various adhesive thicknesses. The ASTM D3528 tests investigated the major parameters, such as adhesive thickness, adherend, and doubler stiffness differences.

The adhesive bonded composite laminate joint was analysed using the finite element method (FEM) and the results were compared to test results. The 2D and 3D FEM model were created reflecting the detailed specimen dimensions (Adherends and various adhesive thicknesses) and test load and boundary conditions (L/BCs).

A progressive failure analysis (PFA) was applied to the FEM to predict the overall failure behavior of the test specimens and failure loads. To analyze the bonding interface failures – such as cohesive failure, adhesive failure, and interlaminar failure the interface stresses distribution between the adhesive and adherend were analyzed in detail with theoretical calculations. The overall behaviour of the FEM and test results were showed by comparing the load versus displacement for the PFA result.

The PFA method was suitable for predicting the test behavior and maximum test load, except for detailed failure modes.

1. Introduction

The use of adhesive on airframe structural joints and in the automotive industry is increasing as a major composite joining method [1], such as by co-bonding or secondary bonding. The thin film adhesive is mostly used for co-bonding or secondary bonding on structural parts.

The relatively thick paste type adhesive is used for secondary bonding or field repair bonding by various methods. There has been improvement, including the theoretical study on strength calculation, FEA method improvement, and a lot of test data. Lucas [2] reviewed and summarized the extensive literatures on the existing analytical model for both adhesive single and double lap joints.

The thick adhesive bonded joint is more complicated compared with the thin adhesive joint due to geometrical and process parameters.

The major parameters for adhesive bonded composite joints are joint type, mechanical property of adhesive, condition of adhesion surface [3], relative strength, and stiffness differences between the adherend and doubler.

This study focuses on the adhesive bonded double lap joint with different adhesive thickness and the paste type adhesive. To evaluate the adhesive properties such as shear strength, elastic and plastic characteristic of adhesive for various thicknesses ASTM D5656 [4] tests were performed. Test results were used to analyze the adhesive boned double lap joint, ASTM D3528 [5]. Adhesive shear stress distribution and failure mode from the FEM result were compared with the test results.

2. Adhesive material & properties

Hysol® EA9394 is widely used to bond the aircraft structures in the aerospace industry. To analyze the shear modulus, strength, and strain, the ASTM D5656 test was performed for various adhesive thicknesses with aluminum adherends. Figure 1 shows the shear stress and strain curve for thicknesses from 0.51 mm (0.02 inch) to 2.03 mm (0.08 inch). These curves represent the elastic-plastic behaviour of adhesive material loading the shear force for the various adhesive thicknesses [6]. Tensile properties, modulus, strength, and elongation were referenced in Table 2 [7].

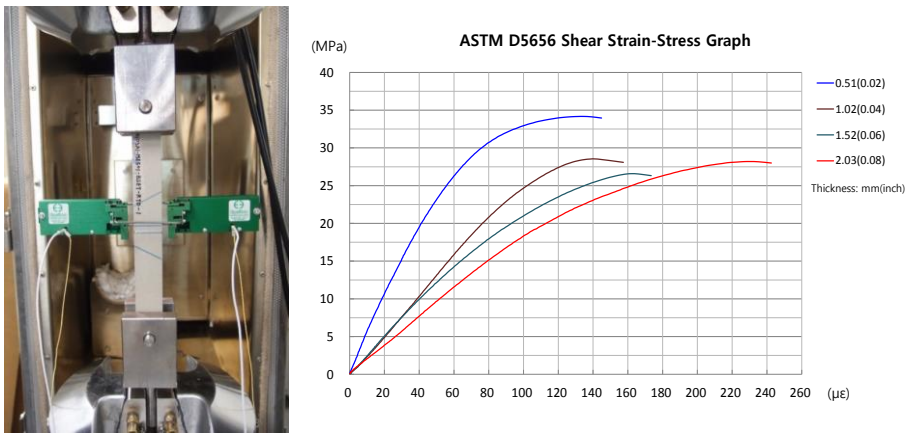

Figure 1. ASTM D5656 adhesive shear test results

Table 1. Shear properties for various adhesive thicknesses

Thickness mm, (inch)	Modulus[1)] (MPa)	Strength (MPa)	Strain (γ^{ult})	Elastic (γ_e)	Plastic (γ_p)
0.51(0.02)	572	34.2	0.14	0.060	0.080
1.02(0.04)	369	29.5	0.15	0.080	0.070
1.52(0.06)	349	26.2	0.17	0.075	0.095
2.03(0.08)	202	28.3	0.24	0.140	0.120
1) Shear Modulus: Chord modulus, $G=(\tau_0 - \tau_{0.01})/(\gamma_0 - \gamma_{0.01})$					

Table 2. Tensile properties

ASTM D638 Tensile test			
Modulus (E), (MPa)	Poisson's ratio(ν)	Strength (MPa)	Failure Strain(ε^{tu})
4481.4	0.37	42	0.018
Butt tensile test			
Adhesive thickness (mm)	0.64	1.27	2.54
Strength (MPa)	47.1	40.9	37.3

CYCOM® 5276-1 G40-800 Tape [8] was used as a base material to make the laminates and test specimens. Table3 shows the experimental results as performed via the ASTM tests.

Table 3. Lamina mechanical properties of adherend and doubler

Properties	Value	Unit	Specification
Axial Modulus, E1	130.5	GPa	D3039
Transverse modulus, E2	9.11	GPa	D3039
Shear Modulus, G12	5.06	GPa	D3518
Axial Tensile Strength, XT	2298	MPa	D3039
Axial Compressive Strength, XC	1373	MPa	D695
Transverse Tensile Strength, YT	72.7	MPa	D3039
Transverse Compressive Strength, YC	234.7	MPa	D695
Shear Strength, τ12	110	MPa	D2344
Poisson's ratio, ν12	0.33		D3039
Density, ρ	1.588	g/cm^3	D792

3. Test matrix specimen IDs

The adhesive thickness is considered as a major parameter effect on the shear strength of an adhesive bonded joint. The adhesive shear strength and butt tensile strength for the various adhesive thickness referenced in Table 1 was used for analysis. The stiffness difference between the adherend and doubler is also included as parameters in Table 4.

Table 4. Test matrix and test IDs

Specimen Type	Adhesive	Adherend	Doubler	Test spec
Adhesive-bonded double lap joint	EA9394 (Paste Adhesive)	CFRP laminate (Various laminates)	CFRP laminate [45/90/-45/0]s	ASTM D3528 Type B
1) Plies : 1 ply = 0.19 mm (0.0075 inch)				
2) TEST ID :	D3528B-T01–A01-01			
TXX	Bonding geometry(Thickness x Length, mm (inch)) 01: 0.51(0.020) x 38.1(1.5) 02: 1.02(0.040) x 38.1(1.5) 03: 1.52(0.060) x 38.1(1.5) 04: 2.03(0.080) x 38.1(1.5)			
AXX	Stacking sequence of adherend laminate 01: [45/90/-45/0/-45/45/-45/45/45/-45]s 02: [45/90/-45/0/-45/45/90/0/45/-45]s 03: [45/90/-45/0/90/0/-45/45]s 04: [45/90/-45/0/90/0/-45/90/45/0]s 05: [45/90/-45/0/90/0/90/0/90/0]s 06: [45/90/-45/0/90/0/-45/0/45/0]s 07: [45/90/-45/0/0/0/-45/0/45/0]s			
XX	Specimen number			

4. Theoretical background

The strength of a double lap joint can be predicted using theoretical and experimental equations . The shear stress (τ) for elastic zone can be expressed as Equation (1), while the constants A and B are described in reference [9].

$$\tau = A\sinh(\lambda x) + B\cosh(\lambda x) \quad (1)$$

The adhesive normal stress, peel stress (σ_{an}) is expressed as Equation (2).

$$\sigma_{an} \cong (E'_c)/t_a \cdot (\tau t_o)/2D \cdot 1/\chi^3 = \tau ((3E'_c \cdot (1-\nu^2))/(E_o \cdot t_a))^{0.25} \quad (2)$$

Where E'_c is the effective tensile modulus of the adhesive, D is the flexural rigidity of adherend. Shear stress distribution for adhesive bondline is used to compare the FEM shear stress output.

5. FEM modeling for numerical analysis

To analyze the double lap adhesive joints on the composite laminates, FEM models were created reflecting the detailed test load and boundary conditions (L/BCs). Total test specimen geometry was created for the FEM models for better understanding and direct comparison with the test result. The 2D FEM model reflected both the composite laminate adherends. The 3D FEM model reflected the adhesive layers having various thicknesses. Figure 2 shows the detail 2D FEM model for the test specimen composed of the 2D FEM and 3D FEM elements.

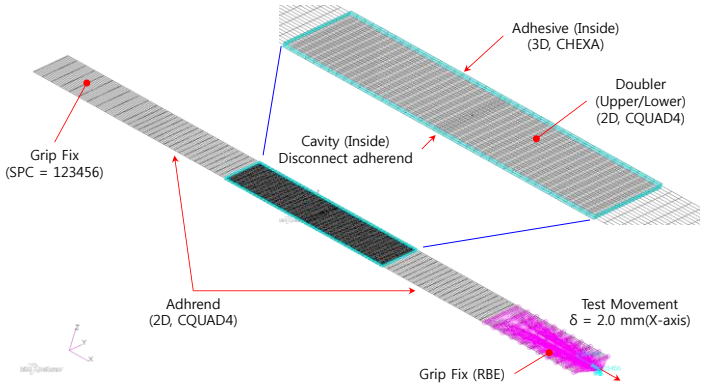

Figure 2. 2D FEM model and L/BCs for specimen

As an FEA analysis method for adhesive bonded joints, other researchers used the cohesive element for the virtual crack closure technology (VCCT) method [10, 11]. This method can simulate the damage and fracture behavior of adhesive joints but additional material properties, such as fracture toughness, are required and the FEM model is complicated.

In this study, to predict the maximum load in the analysis, laminate failure theories and the PFA method (MSC. Nastran solution 400 [12]) were used based on the basic mechanical properties for lamina and adhesive.

For the material degradation model, immediate options were adopted for the analysis. The test result graph shows the instant load drop during the initial and final failure. It represents the brittle adhesive and laminate characteristics.

6. ASTM D3528 test setup and results

ASTM D 3528 test is tensile test. It measures the overall load and displacement for specimen. To measure the local displacement, a strain gage or extensometer was used for the intended area.

To measure the local displacement of both adherends, an additional fixture was designed. Figure 3 shows the test set up with the assembled additional fixture and extensometers. The test load (P) and local displacement (δ) for adherend displacement are collected in Material Testing System (MTS) 810. These data are used to compare with the FEM result as a load-displacement graph.

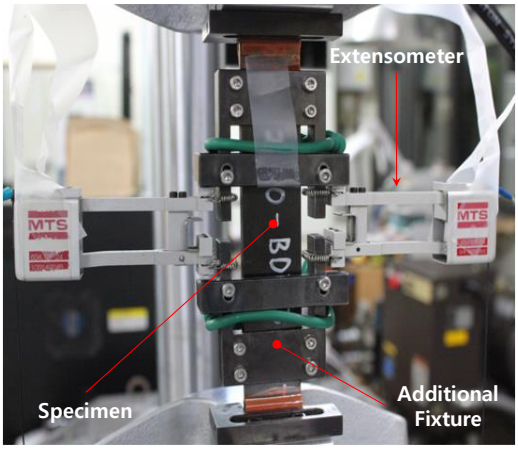

Figure 3. ASTM D3528 Type B Test & Test Fixture

The test results for each specimen were shown as three major failure modes (adhesive failure on the adhesion surfaces, mixed failure, adherend failure). Figure 4 shows the failure images and detail descriptions. The adhesive failure occurs when the adhesion strength in the interface surface is lower than doubler or adherend strength. It also occurs because of the adhesive defects, such as voids or bubbles inside the adhesive layer during the manufacturing. The cohesive failure occurs when the adhesive itself fails during load carry or adhesive defects. The adherend failure, inter-lamina failure occurs when the adherend or doubler fails due to the inter-lamina stress, adhesive peel stress, or surface damage during the surface treatment (such as sanding). Some test results show the adhesive failure with low test loads. Manual sanding treatment (grit 120 sanding paper) work can create non-uniform surface roughness and thus create low adhesive failure. The test results showed that the adhesive shear strength gradually increases with the adherend stiffness increase on the same adhesive thickness specimen.

Failure Images	Failure Code
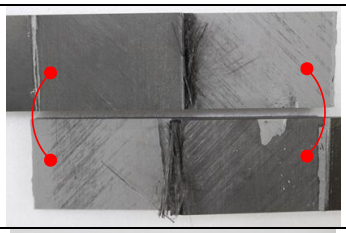	Adhesive fail (Adhesive debond)
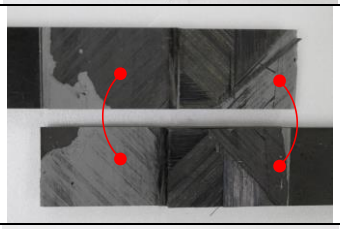	Mixed fail Cohesive + adherend (Adhesive broken) (Adherend delamination)
	Adherend fail (Adherend delamination)

Figure 4. ASTM D3528 failure codes

Table 5. Test matrix and results

Test ID	P_{max} (kN)	τ_{av} (MPa)	Failure	Test ID	P_{max} (kN)	τ_{av} (MPa)	Failure
D3528B-T01–A01	21.3	11.0	Adhesive	D3528B-T03–A01	17.2	8.8	Adhesive
D3528B-T01–A02	28.9	15.0	Mixed	D3528B-T03–A02	25.3	13.2	Adhesive
D3528B-T01–A03	32.2	16.4	Mixed	D3528B-T03–A03	17.0	10.4	Mixed
D3528B-T01–A04	24.8	12.7	Adhesive	D3528B-T03–A04	27.8	14.3	Mixed
D3528B-T01–A05	40.2	20.8	Adhesive	D3528B-T03–A05	31.7	16.2	Mixed
D3528B-T01–A06	35.1	18.0	Adhesive	D3528B-T03–A06	35.7	18.4	Adhesive
D3528B-T01–A07	35.6	18.3	Mixed	D3528B-T03–A07	32.5	16.7	Adhesive
D3528B-T02–A01	21.7	11.2	Adhesive	D3528B-T04–A01	22.4	11.6	Adhesive
D3528B-T03–A02	33.3	17.1	Mixed	D3528B-T04–A02	25.4	13.0	Mixed
D3528B-T03–A03	26.7	9.85	Mixed	D3528B-T04–A03	23.8	12.2	Adhesive
D3528B-T03–A04	26.7	13.7	Adhesive	D3528B-T04–A04	26.7	13.7	Mixed
D3528B-T03–A05	30.6	15.7	Adhesive	D3528B-T04–A05	26.5	13.6	Adhesive
D3528B-T03–A06	27.2	14.0	Mixed	D3528B-T04–A06	28.4	14.7	Adhesive
D3528B-T03–A07	31.2	16.2	Adhesive	D3528B-T04–A07	27.2	14.0	Mixed

7. FEM analysis results and discussion

The 3D FEM analysis results for the D3528-T01-A02 specimen are shown in Figure 5. The FEM result shows the delamination failure with failure index. The failure locations are close to the failure specimen and failure behaviors.

Figure 6 shows the shear stress distributions created from the theoretical calculation in Equation (1) and FEM increment results. The results also show that the shear stress gradually increases and fails first on the both sides of doubler area as the load increases.

Figure 7 show the load-displacement curve for the test results and 2D, 3D FEM results. The initial failure area of the FEM and test results, final failure displacement, and failure load results are similar.

Maximum stress failure criteria is used for both adhesive and composite adherend.

The 2D, 3D FEM results, test maximum loads are summarized and compared in Table 6. The 3D FEM results were added to facilitate a comparison with the 2D FEM results for verification.

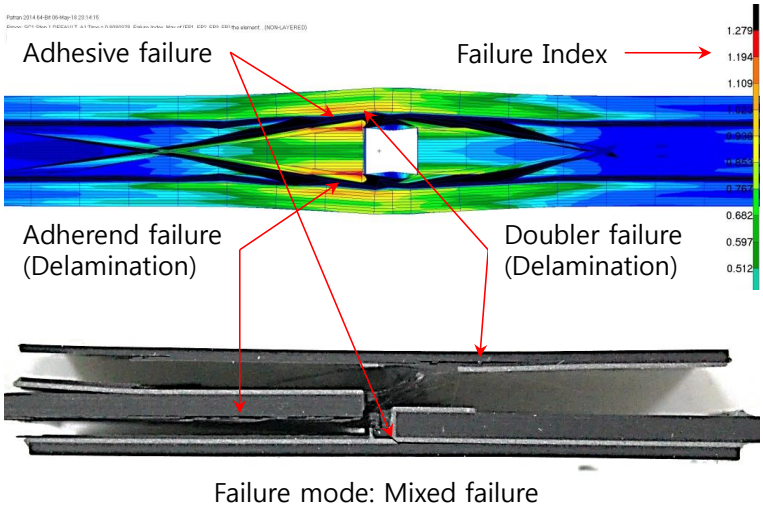

Figure 5. T01–A03 analysis results & failure image

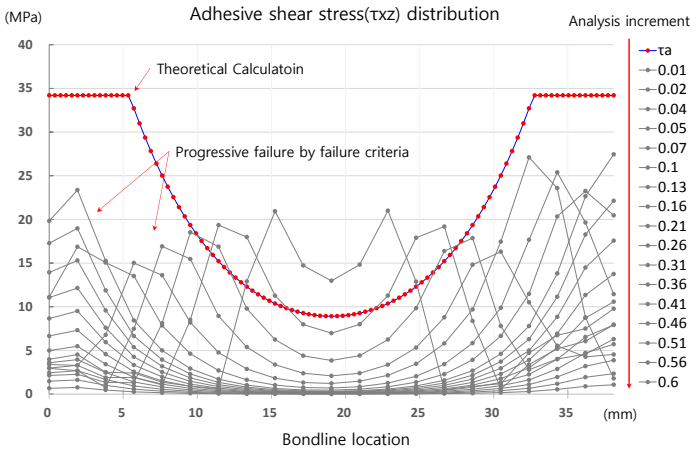

Figure 6. T01–A03 Adhesive shear stress (τxz) result

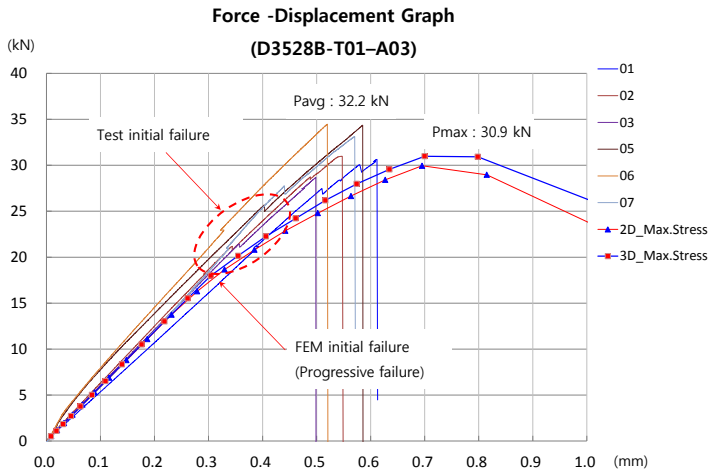

Figure 7. T01-A03 test & FEM result plots

Table 6. Test and FEM results summary

Test ID	P_{max} (kN), (S.D[1)])	FEM(kN)	R.E[2)](%)	Test ID	P_{max} (kN), (S.D[1)])	FEM(kN)	R.E[2)](%)
T01–A01	21.3, (4.1)	28.7(31.0)[3)]	34.4	T03–A01	17.2, (3.5)	27.0	57.6
T01–A02	28.9, (2.9)	30.9(33.8)[3)]	6.8	T03–A02	25.3, (3.8)	28.9	14.2
T01–A03	32.2, (2.2)	29.9(30.9)[3)]	-7.0	T03–A03	17.0, (8.6)	28.2	65.7
T01–A04	24.8, (3.3)	31.9(35.7)[3)]	28.7	T03–A04	27.8, (7.5)	29.8	7.2
T01–A05	40.2, (3.2)	33.7(35.9)[3)]	-16.2	T03–A05	31.7, (1.1)	31.0	-2.3
T01–A06	35.1, (5.1)	33.9(36.6)[3)]	-3.3	T03–A06	35.7, (6.4)	30.8	-13.8
T01–A07	35.6, (2.1)	34.9(37.2)[3)]	-1.9	T03–A07	32.5, (6.0)	30.8	-5.0
T02–A01	21.7, (3.0)	27.9	28.4	T04–A01	22.4, (4.0)	29.5	31.3
T03–A02	33.3, (1.1)	30.1	-9.5	T04–A02	25.4, (6.0)	31.3	23.3
T03–A03	26.7, (6.4)	29.3	10.1	T04–A03	23.8, (3.9)	29.5	24.0
T03–A04	26.7, (4.5)	31.1	16.7	T04–A04	26.7, (4.7)	31.8	19.0
T03–A05	30.6, (6.7)	31.5	2.8	T04–A05	26.5, (6.4)	33.3	25.9
T03–A06	27.2, (0.7)	31.8	17.1	T04–A06	28.4, (4.0)	32.3	13.9
T03–A07	31.2, (4.3)	32.8	3.9	T04–A07	27.2, (3.8)	32.5	19.5

1) S.D (Standard Deviation), kN
2) Relative Error, % : (FEM Pmax –Test Pmax) / Test Pmax
3) 3D FEM Result

8. Conclusion and further study

The total comprehensive procedure for the adhesive bonded joint (ASTM D3528) was demonstrated from the test analysis of the FEA result. The applied PFA method was suitable for predicting the maximum bonding load and strength. The FEM results in Table 6 show failure loads within 30% relative error, except in 4 cases. The 2D and 3D FEM results are similar.

However, the FEM result was not sufficient to represent the detailed failure behavior of the inside adherend inter-laminar failures. The mixed failure can be analyzed when the FEM model and analysis method can analyze the detail failure mechanism for the adhesive and laminate failures including infinitesimal load increments and fracture behaviors.

Acknowledgments

This research was supported under the framework of Aerospace Technology Development Program (No. 10074270, Development of Manufacturing Core Technology for 3-Dimnesional Woven Integrated Composite Wing Structure of 5,000 Pound VLJ Aircraft) funded by the Ministry of Trade, Industry & Energy (MOTIE, Korea)

References

[1] A Higgins. Adhesive bonding of aircraft structures. *International Journal of Adhesion & Adhesives,* 20:367–376, 2000.

[2] Lucas F.M. da Silva, Paulo J.C. das Neves. Analytical models of adhesively bonded joints-Part I:Literature survey. *International Journal of Adhesion & Adhesives,* 29:319–330, 2009.

[3] R. D. Adams. *Adhesive bonding Science, technology and applications*. CRC Press, 2005.

[4] ASTM D5656, Standard Test Method for Thick-Adherend Metal Lap-Shear Joints for Determination of the Stress-Strain Behavior of Adhesives in Shear by Tension Loading. *ASTM International*, 2004.

[5] ASTM D3528, Standard Test Method for Strength Properties of Double Lap Shear Adhesive Joints by Tension Loading. *ASTM International*, 2008.

[6] John Tomblin, Waruna Seneviratne. Shear Stress-Strain Data for Structural Adhesive. *U.S.Department of Transportation Federal Aviation Administration, DOT/FAA/AR-02/97,* 2002

[7] T. R. Guess, E. D. Reedy, M. E. Stavig. Mechanical properties of Hysol EA-9394 structural adhesive. *Sandia Report,* 1995.

[8] CYCOM 5276-1 Technical Data Sheet. https: www.cytec.com.

[9] Hart-Smith. L. J. Adhesive-bonded double-lap joints. *NASA Contractual Report NASA CR-112235*, 1973.

[10] Carlos Sarrado, Frank A. Leone. Finite-thickness cohesive elements for modeling thick adhesives. *Engineering Fracture Mechanics,* 168:105–113, 2016.

[11] J. Neumayer, H. Koerber. An explicit cohesive element combining cohesive failure of the adhesive and delamination failure in composite bonded joints. *Composite Structures,* 146:75–83, 2016.

[12] MSC. Nastran 2014 Nonlinear User's Guide SOL 400.